Eur. Phys. J. D **21**, 191–204 (2002)
DOI: 10.1140/epjd/e2002-00200-6

THE EUROPEAN PHYSICAL JOURNAL D

Time-dependent analysis of tunneling effect in the formation of ultracold molecules via photoassociation of laser-cooled atoms

M. Vatasescu[1] and F. Masnou-Seeuws[2,a]

[1] Institute of Space Sciences, MG-23, 76911 Magurele-Bucharest, Romania
[2] Laboratoire Aimé Cotton, CNRS, bâtiment 505, Campus d'Orsay, 91405 Orsay Cedex, France

Received 19 April 2002
Published online 1st October 2002

Abstract. The paper contains a time-dependent investigation of the tunneling effect observed in the photoassociation spectrum of Cs_2 and attributed to the $0_g^-(6s, 6p_{3/2})$ double well. When by photoassociation of two cold cesium atoms a vibrational level of the outer well is populated, tunneling is an efficient mechanism for transferring the population to the inner well ($R < 15a_0$), where spontaneous emission may lead to formation of cold molecules in low vibrational levels of the $a^3\Sigma_u^+(6s, 6s)$ electronic state. This tunneling effect is analyzed by wavepackets propagation, first considering the double well potential alone, and following a packet made by a superposition of states initially located at large distances. Characteristic times for the vibration dynamics, corresponding to a beating phenomenon between the two wells, to partial "revival" at large distances, and to maxima in the population localized in the inner well are reported and discussed. Second, we simulate the two-channels $a^3\Sigma_u^+(6s, 6s) \rightarrow 0_g^-(6s, 6p_{3/2})$ photoassociation at detunings around 2.9 cm^{-1}: the inner well can be populated either by the excitation of a vibrational level of the external well (resonant excitation), or by tuning the photoassociation laser at the energy of the inner well level which displays tunneling ("off-resonance excitation"). In the first case the photoassociation is efficient, while the tunneling probability is small; in the second, the tunneling probability is large, so that despite the poor efficiency of the photoassociation process, more population can be transferred to the inner well. This second choice is shown to be very sensitive to the laser intensity, which could be used to control the population of the inner well and hence the formation of ultracold molecules in low vibrational levels.

PACS. 03.65.Xp Tunneling, traversal time, quantum Zeno dynamics – 31.15.Qg Molecular dynamics and other numerical methods – 33.80.Ps Optical cooling of molecules; trapping – 33.80.Gj Diffuse spectra; predissociation, photodissociation – 34.30.+h Intramolecular energy transfer; intramolecular dynamics; dynamics of van der Waals molecules

1 Introduction

Formation of ultracold molecules, at temperatures below 10^{-3} K, has received much attention lately due to the demonstration of efficient schemes in samples of cold Cs [1,2], K [3] and Rb [4] atoms. Most schemes rely upon the photoassociation reaction [5], where a molecule is formed in an excited electronic state from a pair of colliding atoms which absorb a photon. The photoassociated molecule decays by spontaneous emission, most often giving back a pair of ground-state atoms and in some particular situations a stable molecule in the ground (or lowest triplet) electronic state. Efficient schemes require a favourable branching ratio between the stabilization and dissociation channels: the search is difficult since the photoassociation reaction preferentially takes place at large internuclear distances (see Fig. 1), forming long range molecules where the two atoms are most of the time very far apart, so that the decay probability to bound levels in the shorter-range ground-state potential is negligible. In the Cs_2 case, it is the presence of double-well structures in the excited $1_u(6s + 6p_{3/2})$ and $0_g^-(6s + 6p_{3/2})$ potential curves which provides good Franck-Condon factors for population of vibrational levels v" of the $X^1\Sigma_g^+$ and $a^3\Sigma_u^+$ electronic states respectively. Generally, the decay step is populating excited vibrational levels v", so that the stable molecule, although "translationally cold", is still "vibrationally hot".

However, formation of ultracold molecules in low vibrational levels v" has also been achieved owing to an unexpected tunneling mechanism. Indeed, in a previous paper [6], we have analyzed two features with larger rotational structures, present in the Cs_2 photoassociation spectrum [7], and reported calculations assigning them to levels of the inner well of the $0_g^-(6s, 6p_{3/2})$ potential populated *via* photoassociation into levels of the outer well and *tunneling* through the barrier. The scheme is recalled

[a] e-mail: francoise.masnou@lac.u-psud.fr

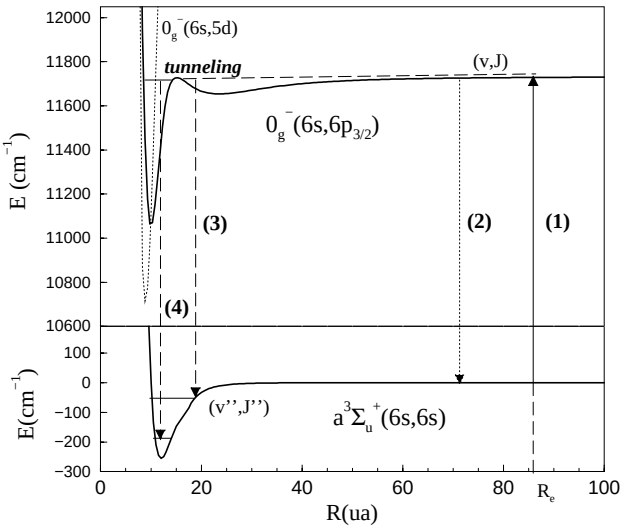

Fig. 1. Electronic potentials involved in the $a^3\Sigma_u^+ \longrightarrow 0_g^-(6s, 6p_{3/2})$ photoassociation of Cs_2 (the $0_g^-(6s, 5d)$ potential which influences the tunneling is also represented with dotted line). The photoassociation reaction is taking place at large distances (1), populating a vibrational level of the outer well. By spontaneous emission, the photoassociated molecule can decay back into a pair of cold atoms (2) or be stabilized in a bound level v" of the lower triplet state (3). After *tunneling*, a level of the inner well is populated, which has good Franck-Condon overlap with the low v" levels (4).

in Figure 1. The tunneling effect, unusual for a heavy molecule like Cs_2, is an efficient mechanism to transfer the population from large distances (still two atoms) to the inner zone, where spontaneous emission can reach very low vibrational levels of the $a^3\Sigma_u^+$ state, creating molecules that are also vibrationally cold (as we indicate by (4) in Fig. 1).

In the present work, our aim is to explore further this tunneling mechanism, now using time-dependent calculations, related to a previous work on the dynamics of the photoassociation reaction [8] in the case of a single-well excited potential. The latter paper showed competition between two characteristic times related to vibration in the potential well and Rabi coupling due to the cw-laser. At small detunings, when vibrational levels close to the dissociation limit are populated, the vibration period can become larger than the Rabi period, creating "strong field situations" where the dynamics can be controlled by the intensity of the laser. We shall answer questions such as:

- Can we associate a characteristic time to tunneling in the photoassociation conditions?
- What is the mechanism to transfer population to vibrational levels of the inner well ($R < 14a_0$) through a photoassociation reaction taking place at large distances ($R \geq 70a_0$)?
- Which proportion of the population in the $0_g^-(6s, 6p_{3/2})$ excited potential can be localized in the inner well at a given time t?
- Is the tunneling effect depending upon the intensity of the photoassociation laser or, in other words, can we control tunneling by varying the intensity?

Some remarks have to be made relative to the first question which refers directly to the very debated concept of *tunneling time*. The variety of approaches around this notion shows that it is considered as meaningful, despite the fact that "this is a field with a diversity of viewpoints, without a clear consensus", as stated in reference [9], which reviews three categories of approaches used to define a time scale associated with the duration of the tunneling process: (i) by following wave packets incident on the barrier, (ii) by determination of a set of dynamic paths $x(t)$ (found through the Feynman path-integral formulation, through the Bohm approach, or through the Wigner distribution) used to ask how long each path spends in the barrier and which is averaged in some way, (iii) by defining a physical clock used to measure the time elapsed during tunneling. Very recently, another paper [10] proposed a definition of tunneling time through a barrier by using the local value of a "time" operator. The authors emphasize that "a universal intrinsic tunneling time that is valid for all experiments probably does not exist. There are most likely a multiplicity of tunneling times in nature, each one describing a different type of experiment". This meets an older remark about the fact that "different expressions for the tunneling time could be relevant under different circumstances" [11]. The approach using wave packets to study tunneling was very probably the context which introduced the question about a tunneling time. In references [9,11,12] can be found definitions of different tunneling times from the deformation of an incident wave packet, as well as discussions of their problematic points and references about this subject. As far as the present work is concerned, the main aim is to modelize time-dependent photoassociation experiments, so that we shall not focus on the definition of a "tunneling time", but rather take a pragmatic approach analyzing the results of wavepacket-propagation calculations and searching for a possible characteristic time related to tunneling.

A wavepacket analysis of tunneling obviously gives results depending upon the choice of the initial wavepacket. As we treat a tunneling effect manifested in the photoassociation of two cold atoms at well-defined resonance energies, we can have an "unambiguous choice" of the initial energy of the wavepacket and of its localization at the interatomic distance where the photoassociation process is taking place. This will be discussed below in Section 4.

The paper is organized as follows: in Section 2 we summarize our previous analysis of the $0_g^-(6s, 6p_{3/2})$ photoassociation spectrum showing the existence of a tunneling effect, and discussing the influence of coupling with another channel, $0_g^-(6s, 5d)$, in the region of the inner well. For clarity sake, we propose in the present work a simplified model where the coupling with this other channel is neglected. In Section 3, we estimate the various characteristic times useful to interpret time-dependent calculations. In Section 4 we report a time-dependent analysis of the tunneling effect in the Cs_2 $0_g^-(6s, 6p_{3/2})$ double well using wavepacket propagation. Section 5 contains the analysis of tunneling effect in the $a^3\Sigma_u^+ \rightarrow 0_g^-(6s, 6p_{3/2})$ photoassociation reaction, when a level of the $0_g^-(6s, 6p_{3/2})$ inner

well can be populated. Section 6 is the conclusion. In a forthcoming paper we shall complete the present work by more sophisticated calculations introducing the coupling with the $0_g^-(6s, 5d)$ channel and estimating the rate of formation of stable molecules by spontaneous emission, in order to give conclusions directly relevant to experiment.

2 Tunneling in the Cs_2 $0_g^-(6s, 6p_{3/2})$ photoassociation spectrum: observed spectrum and simplified model

The first observation of ultra-cold long-lived Cs_2 molecules [1] relies upon the three following steps, also indicated in Figure 1. The molecules are formed by photoassociation in the $0_g^-(6s + 6p_{3/2})$ excited state:

$$\mathrm{Cs}(6s^2\mathrm{S}_{1/2}, F = 4) + \mathrm{Cs}(6s^2\mathrm{S}_{1/2}, F = 4) + \hbar(\omega_0 - \Delta_\mathrm{L}) \rightarrow \mathrm{Cs}_2(0_g^-(6s^2\mathrm{S}_{1/2} + 6p^2\mathrm{P}_{3/2}; v, J)) \quad (1)$$

using a laser red-detuned by Δ_L relative to the D_2 resonance line. Spontaneous emission either gives back a pair of ground state atoms:

$$\mathrm{Cs}_2(0_g^-(6s^2\mathrm{S}_{1/2} + 6p^2\mathrm{P}_{3/2}; v, J)) \rightarrow \mathrm{Cs}(6s^2\mathrm{S}_{1/2}) + \mathrm{Cs}(6s^2\mathrm{S}_{1/2}) + h\nu_2, \quad (2)$$

or leads to the formation of long-lived molecules in the $a^3\Sigma_u^+$ state:

$$\mathrm{Cs}_2(0_g^-(6s^2\mathrm{S}_{1/2} + 6p^2\mathrm{P}_{3/2}; v, J) \rightarrow \mathrm{Cs}_2(^3\Sigma_u^+(6s^2\mathrm{S}_{1/2} + 6s^2\mathrm{S}_{1/2}; v", J")) + h\nu_3. \quad (3)$$

The ground-triplet-state molecules are detected by a resonant two-step photoionisation process, and time-of-flight analysis of the Cs_2^+ ions [1,6,7]. The 0_g^- potential curve displays a double well structure with a hump located around $15a_0$, as indicated in Figure 1 where we have represented potential curves computed by Spies and Meyer [13], matched at large distances to the asymptotic expansion of Marinescu and Dalgarno [14]. In the photoassociation spectrum, vibrational levels from $v_\mathrm{ext} = 0$ to $v_\mathrm{ext} = 132$ are identified [7], corresponding to vibrational motion in the external well of the $0_g^-(6s^2\mathrm{S}_{1/2} + 6p^2\mathrm{P}_{3/2})$ potential. Also present in the experimental spectrum are two structures (denominated G_1 and G_2), corresponding to binding energies -2.14 cm^{-1} and -6.15 cm^{-1}, which are not part of the regular series v_ext, and which have a well-resolved rotational structure (in contrast with their neighbouring lines identified as levels of the outer well). Their larger rotational constants, $B_v^1 = 4.5 \times 10^{-3}$ cm^{-1} and $B_v^2 = 8.1 \times 10^{-3}$ cm^{-1}, are typical of vibrational motion in the region of the inner well. From the definition of the rotational constant as $B_v = \langle\chi_v|\hbar^2/2\mu R^2|\chi_v\rangle$, where $\chi_v(R)$ is the vibrational wavefunction, $\mu = 121135.83$ au the reduced mass for Cs_2, and R the internuclear distance, it is possible to estimate a mean value of the inverse internuclear distance, yielding $\langle R\rangle_1 \approx 14a_0$ and $\langle R\rangle_2 \approx 11a_0$, whereas the hump in the double-well potential is located at $\approx 15a_0$. The observed spectrum and the rotational constants have been simulated by numerical calculations.

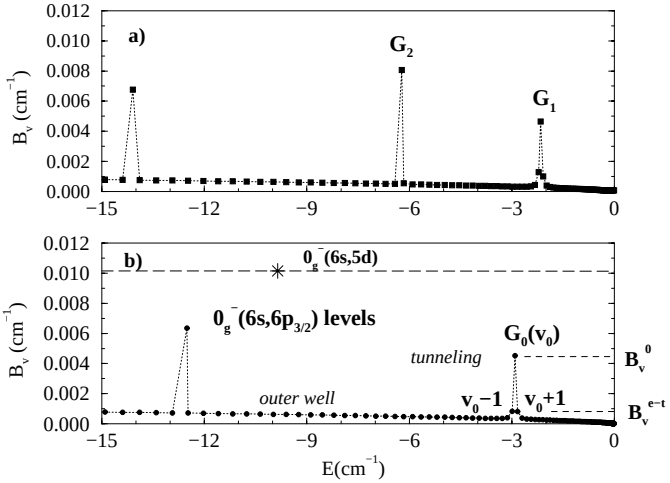

Fig. 2. Rotational constants and energies, for vibrational levels of the $0_g^-(6s, 6p_{3/2})$ and $0_g^-(6s, 5d)$ potentials, computed in reference [6] for $J = 0$. (a) Two coupled channel calculations: the two structures G_1 and G_2 correspond to vibrational levels bound by -2.15 and -6.22 cm^{-1}, with large rotational constants $B_v^1 = 4.64 \times 10^{-3}$ cm^{-1} and $B_v^2 = 8.06 \times 10^{-3}$ cm^{-1}, respectively. In contrast, the levels of the outer well are characterized by small rotational constants. Such calculations agree with experimental results. (b) Two uncoupled channels: vibrational levels of the $0_g^-(6s, 6p_{3/2})$ double well are shown with filled cercles. The G_1 structure is shifted at -2.9 cm^{-1}, giving the G_0 structure corresponding to tunneling in the double well potential. The G_2 structure has disappeared, while a deeper vibrational level of the $0_g^-(6s, 5d)$ potential is indicated by a star.

In reference [6] we have proposed an analysis of these two structures relying on numerical calculation of energies and rotational constants of the $0_g^-(6s, 6p_{3/2})$ vibrational levels using the mapped Fourier grid method [15]. The existence of two structures G_1 and G_2, reported in Figure 2a, is explained both by the tunneling effect and by the coupling in the inner region with the potential $0_g^-(6s, 5d)$ (hereafter referred to as V_d). More precisely, we have compared calculations involving the coupling with the V_d channel with calculations neglecting it. We then can identify the structure G_1 to a vibrational level in the inner well of the $0_g^-(6s, 6p_{3/2})$ potential (G_0 in Fig. 2b), shifted by the coupling with V_d channel, and the structure G_2 to a vibrational level in the V_d potential (indicated by a star in the same figure), shifted by the coupling with the double well potential. Slight modifications of the existing potentials within the expected accuracy of *ab initio* calculations lead to a theoretical spectrum in quantitative agreement with experiment, with two structures G_1 and G_2 having correct binding energies and rotational constants. In contrast, a one-channel model, taking into account only the double well $0_g^-(6s, 6p_{3/2})$ potential, yields a unique structure in the energy domain of the observed spectrum, labeled G_0 in Figure 2b. For qualitative interpretation of the tunneling effect such a model is sufficient, as the position of G_0 is very close (0.06 cm^{-1}) to the observed G_1

Table 1. Energies E_v, rotational constants B_v and vibrational periods for the vibrational levels of the double well having energies around –3 cm^{-1}. v_0 is the level of the inner well, the other levels are located in the external well.

Level	E_v(cm^{-1})	B_v(10^{-3}cm^{-1})	$\hat{R} = (2\mu B_v)^{-1/2}(a_0)$	$T_{\rm vib}^{\rm ext}$(ps)	$T_{\rm vib}^{\rm int}$(ps)
external ($v_0 - 3$)	–3.280	0.36	50.16	218	
external ($v_0 - 2$)	–3.127	0.39	48.19	233	
Ext. + tunneling ($v_0 - 1$)	–2.984	0.83	33.04	210	
Int. + tunneling (v_0)	**–2.904**	**4.5**	**14.19**		3.5
Ext. + tunneling ($v_0 + 1$)	–2.825	0.81	33.44	252	
external ($v_0 + 2$)	–2.693	0.38	48.82	254	

structure. We shall therefore develop in the present paper a simplified model neglecting the weak coupling with the inner $0_g^-(6s, 5d)$ (V_d) potential.

Considering only the $0_g^-(6s, 6p_{3/2})$ double well (see Fig. 3) we shall study the tunneling effect both in the G_0 structure, for the value $J = 0$ of the rotational number, and also in two neighbouring vibrational levels. Indeed, from reference [6], we note that the tunneling effect can be identified from the values of the rotational constant B_v. In the results of time-independent calculations, reported in Figure 2 and in Table 1, the vibrational levels in the external well are characterized by rotational constants $B_v^{\rm ex} \approx 0.4 \times 10^{-3}$ cm^{-1}, there is a level hereafter referred to as v_0 with $B_v^0 = 4.5 \times 10^{-3}$ cm^{-1}, corresponding to a wavefunction mainly localized in the inner well, and two neighbouring levels labeled here $v_0 - 1$ and $v_0 + 1$, with wavefunctions mainly localized in the outer well, but with some probability in the inner well manifested by rotational constants (denoted here as $B_v^{e-t} \approx 2B_v^{\rm ex} \approx 0.8 \times 10^{-3}$ cm^{-1}) slightly larger than the other $v_{\rm ext}$ levels, purely located in the outer well. In the present work, we use a time-dependent approach, assuming that some excitation mechanism (like in the photoassociation process) has created an initial wavepacket at large distances with an energy ~ -3 cm^{-1} relative to the $(6s, 6p_{3/2})$ dissociation limit, close to the binding energy of the G_0 structure, and we follow the time evolution to probe the tunneling dynamics. Two situations are considered:

- first, in Section 4, we treat the one-channel problem of tunneling in the $0_g^-(6s, 6p_{3/2})$ double well, by propagating a Gaussian wavepacket of initial energy ≈ -3 cm^{-1}, *which is a superposition of several vibrational levels surrounding* v_0, from large distances (about $90a_0$) to the inner well;
- second, in Section 5, we study the tunneling mechanism in the photoassociation conditions, *when a single vibrational level of the double well is populated*, and the $0_g^-(6s, 6p_{3/2})$ state is coupled to the continuum of $a^3\Sigma_u^+(6s + 6s)$ by a cw laser. Various detunings are considered, corresponding to resonance either with the v_0 level of the inner well, or with a neighbouring level like $v_0 - 1$.

In both cases, the kinetic energies of the initial Gaussian packets (representing the relative movement of two cesium atoms) are small, in relation with the very low temperatures of the cold collisions.

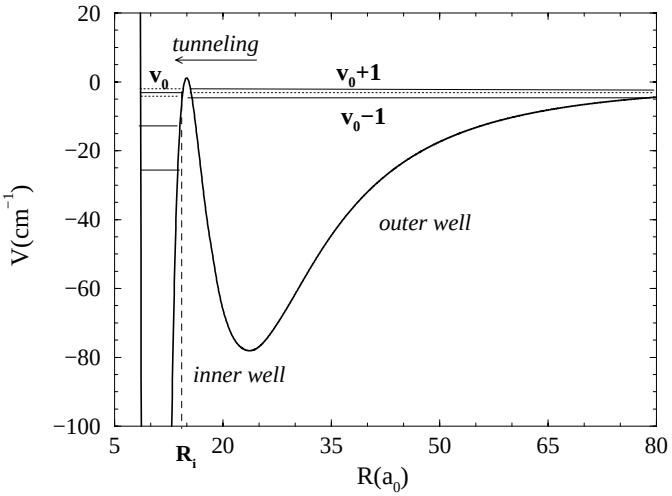

Fig. 3. $0_g^-(6s, 6p_{3/2})$ double well potential. The three last levels in the inner well are indicated in the figure. Tunneling through the barrier is possible for the last vibrational level of the inner well, v_0, and the neighbouring levels $v_0 - 1$, $v_0 + 1$ of the outer well.

3 Characteristic times associated with the dynamics of a pair of cold atoms interacting with laser light

In a previous work on the dynamics of photoassociation [8] in a single-well potential, we remarked that comparing the values of the classical vibrational period in the excited state and Rabi-coupling period gave useful indications for the interpretation of the calculations. The characteristic time $T_{\rm vib}$ is related to the energy difference between two neighbouring vibrational levels of the potential:

$$T_{\rm vib}(E_v) = \frac{2\pi\hbar}{E_{v+1} - E_v} \tag{4}$$

and is close to the classical vibrational period. Considering the problem of the vibrational dynamics in the double-well $0_g^-(6s, 6p_{3/2})$ potential, in the absence of laser coupling, several characteristic times are expected. Since some vibrational levels can be assigned to the outer well (v_e) and others to the inner well (v_0), we can define two characteristic "vibrational periods": one for the levels belonging to the external well, $T_{\rm vib}^{\rm ext}$, and the other for levels of the inner well, $T_{\rm vib}^{\rm int}$. Besides, as already discussed above and recalled above in Table 1, two levels of the external

well have a tunneling wavefunction, so that the level spacing is modified. As reported in the table, the characteristic time $T_{\rm vib}^{\rm ext}$ is in the range 200–250 ps for vibrational levels lying between –3.3 and –2.7 cm^{-1} in the external well, verifying the expected scaling law for a R^{-3} potential $T_{\rm vib}(E_v^{\rm ext}) \sim E_v^{-5/6}$ [8]. The two levels (v_0+1) and (v_0-1) have a modified characteristic time. In the inner well, due to a larger level spacing around 9.5 cm^{-1}, the vibration period is much smaller: we find $T_{\rm vib}^{\rm int} = 3.5$ ps. Moreover, as we show in our calculations presented in Sections 4 and 5, the possibility of tunneling between the two wells around v_0 reveals that a "beating time" between the two wells, defined as:

$$T^{\rm int,ext} = \frac{2\pi\hbar}{E(v_0) - E(v_0-1)} \approx \frac{2\pi\hbar}{E(v_0+1) - E(v_0)} \quad (5)$$

has significance. The value of this third characteristic time is $T^{\rm int,ext} = 420$ ps.

When the photoassociation laser is tuned, we have to solve a two-channels problem in which the electronic potentials $a^3\Sigma_u^+(6s,6s)$ (ground state g) and $0_g^-(6s,6p_{3/2})$ (excited state e) are coupled by the light field with frequency $\omega/2\pi$, $\omega = \omega_0 - \Delta_{\rm L}$. At resonance, the cw-laser is red-detuned by $\hbar\Delta_{\rm L} \sim 3$ cm^{-1} from the energy $\hbar\omega_0$ of the atomic transition $6s \rightarrow 6p_{3/2}$. The time-dependent Schrödinger equation for the two coupled channels is written:

$$\hat{\mathbf{H}}\Psi(t) = (\hat{\mathbf{H}}_{\rm mol} + \hat{\mathbf{W}}(t))\Psi(t) = {\rm i}\hbar\frac{\partial}{\partial t}\Psi(t). \quad (6)$$

The molecular Hamiltonian $\hat{\mathbf{H}}_{\rm mol} = \hat{\mathbf{T}} + \hat{\mathbf{V}}_{\rm el}$ is the sum of the kinetic energy operator $\hat{\mathbf{T}}$ and electronic potential energy operator $\hat{\mathbf{V}}_{\rm el}$, and the coupling term is written in the dipole approximation:

$$\hat{\mathbf{W}}(t) = -\mathbf{D}(\mathbf{r}_i)\cdot\mathbf{e}_{\rm L}E_0\cos(\omega_{\rm L}t), \quad (7)$$

involving the transition dipole moment of the dimer $\boldsymbol{D}(\mathbf{r}_i)$ and the electric field $\mathbf{E} = \mathbf{E}_0\cos(\omega_{\rm L}t) = \mathbf{e}_{\rm L}E_0\cos(\omega_{\rm L}t)$, with amplitude E_0, polarisation $\mathbf{e}_{\rm L}$, and frequency $\omega_{\rm L}/2\pi$.

The explicit temporal dependence of the Hamiltonian $\hat{\mathbf{H}}$ is eliminated in the framework of the rotating wave approximation, which allows to write the radial coupled equations as:

$${\rm i}\hbar\frac{\partial}{\partial t}\begin{pmatrix}\Psi_\Sigma(R,t)\\ \Psi_{0_g^-}(R,t)\end{pmatrix} = \begin{pmatrix}\hat{\mathbf{T}}+\hat{\mathbf{V}}'_\Sigma(R) & \hbar\Omega\\ \hbar\Omega & \hat{\mathbf{T}}+\hat{\mathbf{V}}'_{0_g^-}(R)\end{pmatrix}\begin{pmatrix}\Psi_\Sigma(R,t)\\ \Psi_{0_g^-}(R,t)\end{pmatrix} \quad (8)$$

where the potentials are now crossing and referred to $\hbar\Delta_{\rm L} = 0$ origin:

$$\hat{\mathbf{V}}'_\Sigma(R) = \hat{\mathbf{V}}_\Sigma(R) - \hbar\Delta_{\rm L}, \quad \hat{\mathbf{V}}'_{0_g^-}(R) = \hat{\mathbf{V}}_{0_g^-}(R) - \hbar\omega_0. \quad (9)$$

The period $T_{\rm Rabi}$ of the "Rabi oscillations" is associated with the coupling $\hbar\Omega$ induced by the laser between the two states:

$$T_{\rm Rabi} = \frac{\pi}{\Omega}\cdot \quad (10)$$

Being related to the molecular transition dipole moment $\boldsymbol{D}_{ge}(R)$ between the ground and excited electronic states, the coupling term is R-dependent ($\hbar\Omega(R) = -\boldsymbol{D}_{ge}(R)\cdot\mathbf{E}_0/2$). Since the photoassociation reaction occurs at large distances, we can use the asymptotic value of the dipole moment $\boldsymbol{D}_{ge}(R)\cdot\mathbf{e}_{\rm L} \approx D_{ge}^{\mathbf{e}_{\rm L}}$ deduced from standard long-range calculations [16]. For this reason, the formulae (8, 10) are written for a constant coupling:

$$\hbar\Omega = -\frac{1}{2}\sqrt{\frac{2I}{c\epsilon_0}}D_{ge}^{\mathbf{e}_{\rm L}} \quad (11)$$

where I is the laser intensity. Depending upon the laser intensity and the detuning, we can have different ratios of these characteristic times and, from the discussion in reference [8], we should expect three possible regimes: $T_{\rm vib}^{\rm ext} \gg T_{\rm Rabi}$ "strong coupling", $T_{\rm vib}^{\rm ext} \ll T_{\rm Rabi}$ "weak coupling", $T_{\rm vib}^{\rm ext} \approx T_{\rm Rabi}$ "intermediate coupling". The ratio $T_{\rm vib}/T_{\rm Rabi}$ is increasing when the intensity is increased or the detuning is decreased. For a typical intensity of ≈ 150 W/cm^2, in linear polarisation, the corresponding Rabi period is ≈ 640 ps, larger than $T_{\rm vib}^{\rm ext}$, so we are not in the strong coupling case. The vibration period in the inner well is more than one order of magnitude smaller, so it is certainly a weak coupling case. In contrast, it is interesting to note that this Rabi period is of the same order of magnitude as the beating period $T^{\rm int,ext} = 420$ ps defined above.

4 Time-dependent analysis of the tunneling effect in the Cs_2 $0_g^-(6s,6p_{3/2})$ double well

We shall describe now the results obtained by solving numerically the time-dependent Schrödinger equation for the 0_g^- double well potential:

$$(T + V_{0_g^-})\Psi_{0_g^-}(R,t) = {\rm i}\hbar\frac{\partial\Psi_{0_g^-}(R,t)}{\partial t} \quad (12)$$

with an initial condition $\Psi_{0_g^-}(R, t=0)$, on a spatial grid extending from R_0 to L. The time propagation uses a Chebychev expansion of the evolution operator $\exp(-{\rm i}Ht/\hbar)$ [17], the wavefunctions being introduced through their Fourier grid representation [18].

4.1 Choice of the observables

We shall use several observables to analyze the dynamics:

- snapshots of the $0_g^-(6s,6p_{3/2})$ wavepacket, denoted $\Psi_{0_g^-}(R,t)$, at different times, in order to follow the population transfer from the outer to the inner well when moving under the barrier (at $R \approx 15a_0$);

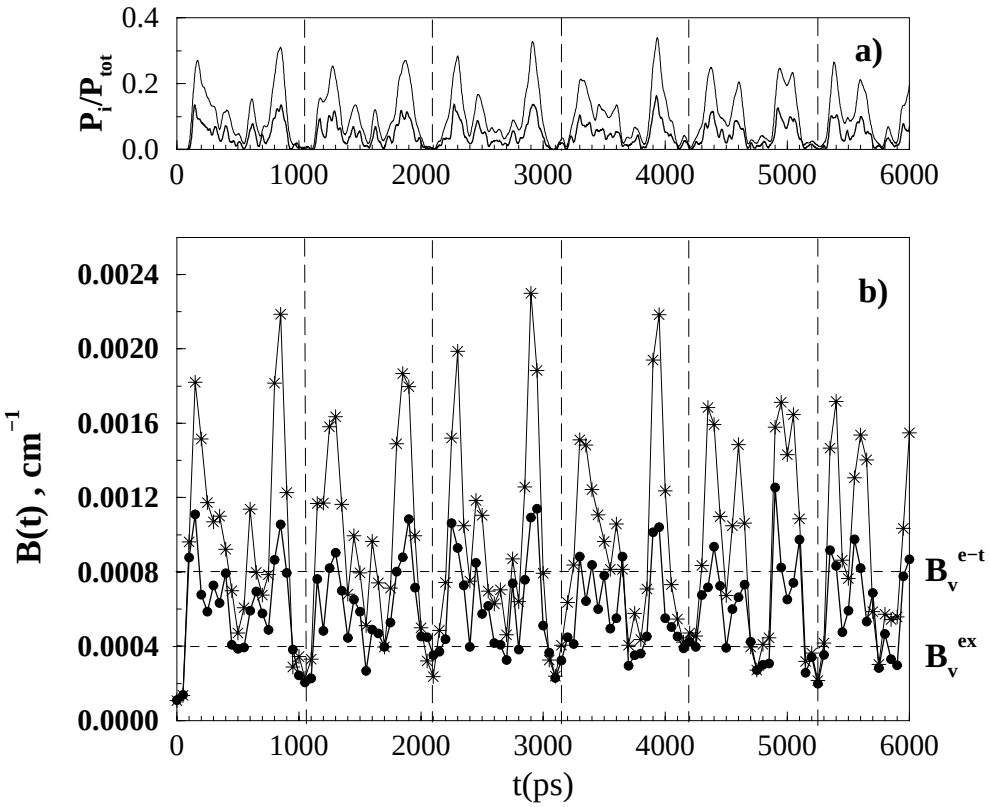

Fig. 4. (a) Time variation of the population in the inner well of the $0_g^-(6s, 6p_{3/2})$ potential during wavepacket propagation ($P_{\rm tot} = P_{0_g^-} = 1$). The thin line represents the result for tunneling at $E = -2.9$ cm^{-1} (initial packet with $p_0 = -0.012$ au, $\Delta p(0) = 0.33$ au). The thick line shows the result for tunneling at $E = -3$ cm^{-1} (initial packet with $p_0 = -0.012$ au, $\Delta p(0) = 0.1$ au). (b) Time variation of $B(t)$ – "rotational constant of the wavepacket" (stars and cercles at intervals of 50 ps correspond to calculated values of $B(t)$ from the packet $\Psi_{0_g^-}(R,t)$). Thin lines and stars for tunneling at -2.9 cm^{-1}; thick lines and filled cercles for tunneling at $E = -3$ cm^{-1}. The horizontal dashed lines show the values of characteristic rotational constants for levels of the outer well ($B_v^{\rm ex} \approx 0.4 \times 10^{-3}$ cm^{-1}) and for the levels $v_0 - 1$, $v_0 + 1$ of the outer well with tunneling ($B_v^{e-t} \approx 0.8 \times 10^{-3}$ cm^{-1}). The vertical dashed lines indicate the values of $t = T_{\rm rev}(v_0 - 1)N/4 = 1\,050$, $2\,100$, $3\,150$, $4\,200$, $5\,250$ ps.

- snapshots of the $0_g^-(6s, 6p_{3/2})$ wavepacket in momentum space, $\Psi_{0_g^-}(p,t)$, since the outer well corresponds to small values of the momentum and the inner well to large values;
- evolution of the population $P_i(t)$ located in the inner well:

$$P_i(t) = \int_{R_0}^{R_i} |\Psi_{0_g^-}(R,t)|^2 {\rm d}R. \qquad (13)$$

At a given energy, R_i is the classical outer turning point in the inner well, as showed in Figure 3. The total population in the $0_g^-(6s, 6p_{3/2})$ channel is:

$$P_{0_g^-} = \left\langle \Psi_{0_g^-} | \Psi_{0_g^-} \right\rangle = \int_{R_0}^{L} |\Psi_{0_g^-}(R,t)|^2 {\rm d}R. \qquad (14)$$

For the one channel case discussed in this section, this population is the total population of the problem, normalized so that $P_{\rm tot} = P_{0_g^-} = 1$;

- expectation value of the *"time-dependent rotational constant"*:

$$B(t) = \left\langle \Psi_{0_g^-}(R,t) \left| \frac{1}{2\mu R^2} \right| \Psi_{0_g^-}(R,t) \right\rangle \Big/ \left\langle \Psi_{0_g^-} | \Psi_{0_g^-} \right\rangle \qquad (15)$$

(the scalar product implies here R-integration on the whole grid, from R_0 to L). This quantity (see Fig. 4) gives information on the location of the wavepacket at a given time t. It is very useful as it can be compared with the results of time-independent calculations reported in Table 1, yielding stationary values $B_v = \langle \chi_v(R) | \frac{1}{2\mu R^2} | \chi_v(R) \rangle$ for the rotational constants of the vibrational levels. The quantity $B(t)$ will have a temporal behaviour similar to the inner well population $P_i(t)$ (with maxima when the population is located at small distances), but its interpretation is easier because of the R^{-2} factor and the normalization in the formula (15).

4.2 Choice of the initial wave packet

We assume that there is a vibrational population in the $0_g^-(6s, 6p_{3/2})$ potential, initially localized at large distances as it is the case in the photoassociation of cold atoms, which can reach the inner well by tunneling. To simulate this, we consider the propagation of a Gaussian packet centered at R_0, with initial momentum p_0, and spatial width $\Delta R(0)$:

$$\Psi(R,0) = \left(\frac{1}{2\pi(\Delta R(0))^2}\right)^{1/4} \mathrm{e}^{\mathrm{i}p_0(R-R_0)} \mathrm{e}^{-\left(\frac{R-R_0}{2\Delta R(0)}\right)^2}. \tag{16}$$

The parameters are chosen so that the energy $E_{\mathrm{init}} = \langle\Psi(R,0)|T + V_{0_g^-}|\Psi(R,0)\rangle$ is close to the "tunneling energies " around –3 cm^{-1}, while the distance R_0 is close to $91a_0$ (*i.e.* the classical outer turning point of the potential at this energy). The packet will describe a superposition of vibrational states. For this precise localization R_0 in the 0_g^- potential, and a small initial momentum p_0, we choose the width $\Delta R(0)$ of the packet (or $\Delta p(0)$ in momentum, with $\Delta p(0)\Delta R(0) = 1/2$ in atomic units) to obtain the desired value of the initial energy. Since the initial momentum p_0 is chosen very small, it is actually the width of the packet that determines the initial energy. We show here calculations for $p_0 = 0.012$ au, to keep the connection with the further simulation of the photoassociation conditions presented in Section 5, but another choice of p_0 does not change the results as long as this value remains smaller than the width $\Delta p(0)$. The reason is that a packet with an initial width $\Delta p(0)$ contains much larger momentum components, $|p| \leq 4\Delta p(0)$ au, which have a determinating influence because they tunnel more easily. For instance, an initial width $\Delta R(0) = 5a_0$ in position, corresponding to $\Delta p(0) = 0.1$ au in momentum, gives the initial energy $E_{\mathrm{init}} = -3.047$ cm^{-1}, close to the energy of the vibrational level $v_0 - 1$ at –2.984 cm^{-1}. The initial distributions in position and momentum are shown in Figure 5: at $t = 0$, the momentum distribution is confined at values $|p| \leq 0.4$ au. In contrast, the motion in the two wells of the 0_g^- potential corresponds to much larger values of momentum, namely up to 10 au in the external well, and from 10 to 30 au in the deep inner well (as it can be seen in the left column of the Fig. 5). We then work with initial packets having momentum distributions very narrow compared to the total momentum domain implied in the problem, which can be considered as a guarantee of stability of the results relative to the choice of the initial packet. Different initial packets, all having small initial kinetic energies, will not change the tunneling results at a given E_{init}. Even if we modify the parameters in equation (16) to probe another value of E_{init} allowing tunneling, the initial wavepacket is keeping its localization at large distance and the confinement in a thin domain of small momenta. For example, we can probe the energy $E_{\mathrm{init}} = -2.906$ cm^{-1}, which is approximately the energy of the inner well level v_0, by a wavepacket with $\Delta R(0) = 1.5a_0$, which means $\Delta p(0) = 0.33$ au.

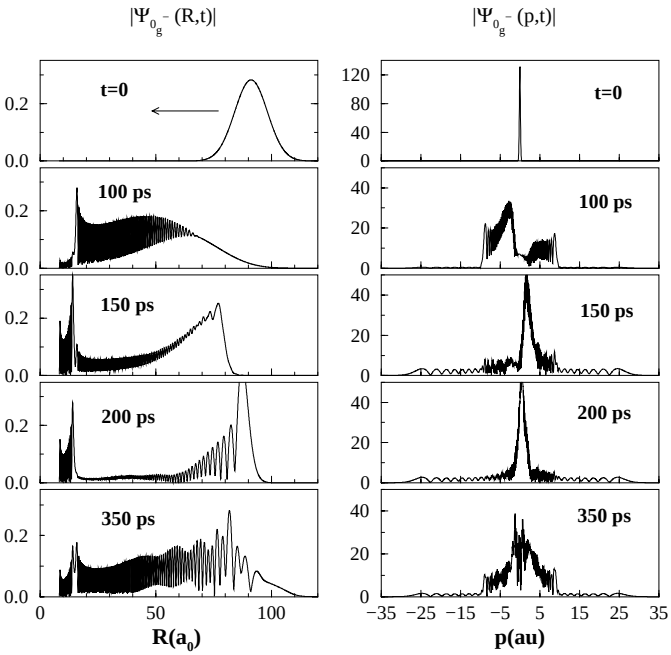

Fig. 5. Time evolution of the wavepackets in the $0_g^-(6s, 6p_{3/2})$ double well, between 0 and 350 ps (initial energy ≈ -3 cm^{-1}). Left column: position space. Right column: momentum space.

4.3 Results

We shall analyze the time-dependent results obtained from the propagation of the wavepackets with initial energies –3 and –2.9 cm^{-1}, allowing tunneling to the inner well. Figures 4a and 4b show that the time-dependent behaviour of the inner well populations P_i and of the "rotational constants" $B(t)$ is very similar for tunneling at –3 cm^{-1} (initial packet with $\Delta p(0) = 0.1$ au, centered at the energy of level $(v_0 - 1)$) and –2.9 cm^{-1} (initial packet with $\Delta p(0) = 0.33$ au, centered at the energy of level v_0). The difference is coming, as expected, from the increased "efficiency" of the tunneling at –2.9 cm^{-1}, due to the resonance with the inner well level v_0, and is manifested by a twice larger filling of the inner well, such that up to 30% of the total population can be transferred.

Figures 5 and 6 display the wavepackets at different instants between 0 and 1 150 ps, during propagation with initial energy $E_{\mathrm{init}} = -3.047$ cm^{-1}, in the position space (left column) and in the momentum space (right column). We can see that between 100 and 150 ps the population of the inner well reaches a maximum. At –2.9 cm^{-1} it takes a slightly longer time to reach the maximum occupation of the inner well (see Fig. 4a), because this maximum is increased. We are tempted to use here the name "tunneling time" for a significant quantity related to an important transfer of population from one well to the other. In this sense, it is possible to identify a time of 50–100 ps as being a duration for under-barrier transit after which the inner well can be either filled up to a maximum or emptied. This characteristic time is visible in Figure 4 on the inner well populations $P_i(t)$, on $B(t)$ for values $B(t) > B_v^{e-t}$,

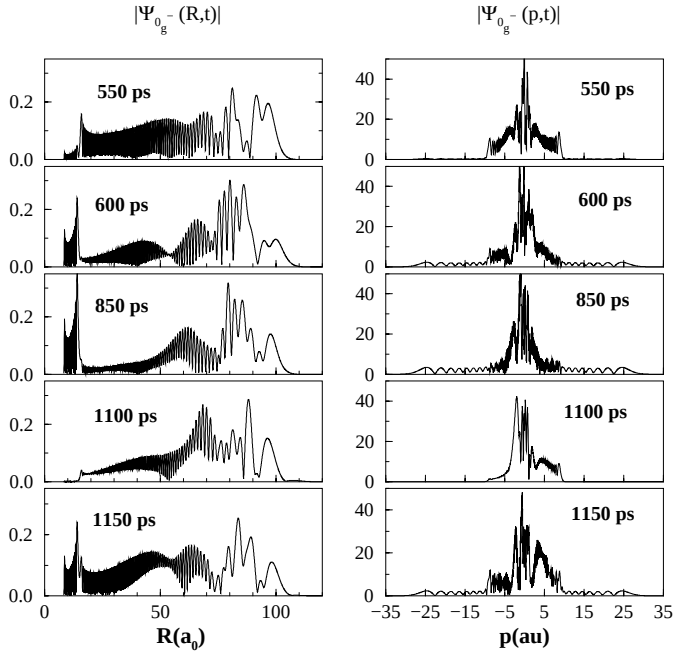

Fig. 6. Time evolution of the wavepackets in the $0_g^-(6s, 6p_{3/2})$ double well, between 550 and 1 150 ps. Left column: position space. Right column: momentum space.

and on wavepackets (for example, 100–150 ps, 550–600 ps, or 1 100–1 150 ps).

A periodicity can be observed in the evolution of the populations $P_i(t)$ and rotational constants $B(t)$: the inner well population goes to 0 at 1 100, 2 100, 3 100, 4 200, 5 250 ps (when the wavepacket leaves the barrier region for larger distances, see for example Figure 6 for $t = 1\,100$ ps), and becomes very small around 550, 1 550, 2 600, 3 650, 4 700, 5 800 ps (when the inner well is almost emptied, but there is population in the outer well in the zone of the barrier, as it can be seen on wavepackets in Fig. 6 for $t = 550$ ps). We shall check an explanation for this pattern using an analysis of the wavepacket as a superposition of several neighbouring vibrational states, manifesting periodic structures in the long-term evolution, due to revivals and fractional revivals of the initial wavepacket, as is shown in reference [19]. It is important to observe that we are not in the conditions discussed in [19], since our problem includes tunneling, and since the packet contains a small number of discrete states, both leading to strong nonclassical behaviour. We therefore do not expect total revival of the initial packet, but a periodic return of the wavepacket to the large distance region, leaving the inner well empty, could account for the minima observed in Figure 4.

It is not trivial to write a time-dependent wavefunction for a problem implying tunneling. In an analytic time-dependent perturbation approach [20] the tunneling transition is said to be occurring due to some time-dependent perturbing term of the Hamiltonian within the barrier. We shall write the wavepacket $\Psi_{0_g^-}(R,t)$ as a function of several eigenstates $\{\chi_v(R)\}$ of the Hamiltonian corresponding to the $0_g^-(6s, 6p_{3/2})$ potential, including the inner well level with a time-dependent coefficient accounting for the fact that it is populated due to a time-dependent perturbation (tunneling):

$$\Psi_{0_g^-}(R,t) \approx \Psi_e(R,t) + c_{v_0}(t)\mathrm{e}^{-\frac{\mathrm{i}}{\hbar}E_{v_0}t}\chi_{v_0}(R) = \sum_{v_e} c_{v_e}(t)\mathrm{e}^{-\frac{\mathrm{i}}{\hbar}E_{v_e}t}\chi_{v_e}(R) + c_{v_0}(t)\mathrm{e}^{-\frac{\mathrm{i}}{\hbar}E_{v_0}t}\chi_{v_0}(R). \quad (17)$$

At $t = 0$ there is no probability amplitude in the inner well, so we have to consider $c_{v_0}(0) = 0$: only *after tunneling* the inner well level v_0 can be manifested in the superposition with a probability $|c_{v_0}(t)|^2$. From $t = 0$ and until the tunneling becomes active, $\Psi_{0_g^-}(R,t)$ is given by the sum $\Psi_e(R,t)$ coming from levels $\{v_e\}$ of the external well. We denote by v_e the vibrational number in the external well, *i.e.* the number of nodes of the wavefunctions in the external well. We shall consider that the sum $\sum_{v_e}$ is strongly weighted around a mean value $\bar{v}_e$. As the initial energies of the packets are ≈ -3 cm^{-1} and –2.9 cm^{-1}, we can suppose that $\bar{v}_e$ corresponds to the level designed as $v_0 - 1$. We suppose that one can expand the energies of v_e levels as a Taylor series around $E_{\bar{v}_e}$:

$$E_{v_e} \approx E_{\bar{v}_e} + \frac{2\pi\hbar}{T_{\mathrm{cl}}(\bar{v}_e)}(v_e - \bar{v}_e) \pm \frac{2\pi\hbar}{T_{\mathrm{rev}}(\bar{v}_e)}(v_e - \bar{v}_e)^2 + ... \quad (18)$$

We used the notations generally termed in the literature [19] as the classical period $T_{\mathrm{cl}}(v_e)$ (which coincides with $T_{\mathrm{vib}}^{\mathrm{ext}}(v_e)$ defined previously) and the revival period $T_{\mathrm{rev}}(v_e)$:

$$T_{\mathrm{cl}}(v_e) = \frac{2\pi}{\omega_{\mathrm{cl}}(E_{v_e})} = \frac{2\pi\hbar}{E_{v_e+1} - E_{v_e}},$$
$$T_{\mathrm{rev}}(v_e) = 2T_{\mathrm{cl}}(v_e)\left|\hbar\frac{\partial\omega_{\mathrm{cl}}}{\partial E}\right|^{-1} \quad (19)$$

with $\hbar\omega_{\mathrm{cl}}(E_{v_e}) = \hbar\omega_{v_e+1,v_e} = E_{v_e+1} - E_{v_e}$, and

$$\frac{\partial\hbar\omega_{\mathrm{cl}}}{\partial E} = \frac{\hbar\omega_{v_e+1,v_e} - \hbar\omega_{v_e,v_e-1}}{\hbar\omega_{\mathrm{cl}}(v_e)}\,. \quad (20)$$

The sign $\pm$ in (18) depends on the sign of the $\partial\omega_{\mathrm{cl}}/\partial E$. Here the presence of v_0 introduces a discontinuity, making $\hbar\omega_{\bar{v}_e+1,\bar{v}_e} > \hbar\omega_{\bar{v}_e,\bar{v}_e-1}$, so the sign is positive for $v_e < \bar{v}_e$ and negative if $v_e > \bar{v}_e$.

We shall develop the analysis in two steps.

(a) The first one deals with the specific dynamics in the external well, independent of tunneling, which periodically brings back the population at large distances. We begin by considering only the packet $\Psi_e(R,t)$ in the external well, without tunneling. It can be written as:

$$\Psi_e(R,t) = \sum_k c_k\chi_k(R)\mathrm{e}^{-2\pi\mathrm{i}(k/T_{\mathrm{cl}} + k^2/T_{\mathrm{rev}})t} \quad (21)$$

with $k = v_e - \bar{v}_e$, and the classical and revival periods having values corresponding to $v_0 - 1$: $T_{\mathrm{cl}} = 210$ ps,

$T_{\rm rev} = 4\,200$ ps. Obviously, for $t = NT_{\rm rev}$, with N integer, $\Psi_e(R,t)$ will recover its initial shape ("revival"). Moreover, reference [19] is demonstrating that for $t \approx T_{\rm rev}(m/n)$, with m/n a rational number, the wavepacket (21) is subject to a sequence of reconstructions, with the probability density determined by the shape of the initial packet, phenomenon called "fractional revival". For example, for $t \approx T_{\rm rev}/2$:

$$\Psi_e(R,t) = \Psi_{\rm cl}\left(R, t + \frac{T_{\rm cl}}{2}\right) \tag{22}$$

and for $t \approx T_{\rm rev}/4$ (and similarly for $3T_{\rm rev}/4$):

$$\Psi_e(R,t) = \frac{1}{\sqrt{2}}\left[{\rm e}^{-{\rm i}\pi/4}\Psi_{\rm cl}(R,t) + {\rm e}^{{\rm i}\pi/4}\Psi_{\rm cl}\left(R, t + \frac{T_{\rm cl}}{2}\right)\right]. \tag{23}$$

In reference [19] $\Psi_{\rm cl}(R,t)$ describes the packet in an early stage of evolution, when $t \ll T_{\rm rev}$ so that the term in $k^2 t/T_{\rm rev}$ can be discarded:

$$\Psi_{\rm cl}(R,t) = \sum_k c_k \chi_k(R) {\rm e}^{-2\pi {\rm i} k t/T_{\rm cl}}. \tag{24}$$

In our case $T_{\rm rev} = 20T_{\rm cl}$, so for $t \approx T_{\rm rev}/4$, we have $\Psi_{\rm cl}(t) = \Psi_{\rm cl}(0)$ and $\Psi_{\rm cl}(t + T_{\rm cl}/2) = \Psi_{\rm cl}(T_{\rm cl}/2)$. The interesting point is that $T_{\rm cl}/2 = 105$ ps, which is just at the beginning of the tunneling manifestation, as it can be seen on the figures showing inner well populations and wavepackets evolution (for example $|\Psi_{\rm cl}(R, T_{\rm cl}/2)|$ can be imagined as having a shape close to the $|\Psi_{0_g^-}(R, t = 100\ {\rm ps})|$ in the Fig. 5). We can then reach the conclusion that "fractional revivals" in the evolution of the $\Psi_e(R,t)$ at $t \approx NT_{\rm rev}/4$ (N integer and $T_{\rm rev}/4 = 1\,050$ ps) keep the population approximately out of the barrier and the inner well (see the wavepacket at 1 100 ps).

(b) Coming back to the time-evolution with tunneling, the expression (15) of $B(t)$ can be written taking into account the development of the packet $\Psi_{0_g^-}$ and specifying the contributions coming from the $\{v_e\}$ levels and the inner well level v_0:

$$\begin{aligned}\left\langle \Psi_{0_g^-} | \Psi_{0_g^-} \right\rangle B(t) &= \left\langle \Psi_{0_g^-}(R,t) \left| \frac{1}{2\mu R^2} \right| \Psi_{0_g^-}(R,t) \right\rangle \\ &= \sum_{v_e} |c_{v_e}(t)|^2 B_{v_e} + |c_{v_0}(t)|^2 B_{v_0} \\ &+ \sum_{(v_e, v_e'), v_e \neq v_e'} \left(c_{v_e}(t) c_{v_e'}^*(t) B_{v_e' v_e} {\rm e}^{-\frac{\rm i}{\hbar}(E_{v_e} - E_{v_e'})t} + {\rm c.c.} \right) \\ &+ \sum_{v_e} \left(c_{v_e}(t) c_{v_0}^*(t) B_{v_e v_0} {\rm e}^{-\frac{\rm i}{\hbar}(E_{v_e} - E_{v_0})t} + {\rm c.c.} \right) \end{aligned} \tag{25}$$

where the c.c. in the parenthesis indicates the summation with the complex conjugated term. In the one-potential propagation, the total population $\langle \Psi_{0_g^-} | \Psi_{0_g^-} \rangle = 1$. The first two terms in the sum (25) contain the rotational constants B_{v_e}, B_{v_0}, and in the last two sums appears the beating between levels of the outer well (v_e, v_e') and between outer well levels v_e and the inner well level v_0. We used the notation $B_{vv'} = \langle \chi_v(R) | \frac{1}{2\mu R^2} | \chi_{v'}(R) \rangle$, where $v \neq v'$ can be v_e, v_e', v_0 (obviously $B_{v_e v_e'} \ll B_{v_e v_0}$). The time-dependence in (25) looks quite complicated, but we can suppose that tunneling implies only the v_0-1, v_0 and v_0+1 levels, and that the last summation contains only contributions from v_0-1 and v_0+1 with a "beating time" $T^{\rm int,ext}$ between the two wells as shown by the formula (5). We can write a simplified formula supposing the coefficients c_v as being real and using the expansion (18). Equation (25) becomes:

$$\begin{aligned} B(t) &= \sum_{v_e} |c_{v_e}(t)|^2 B_{v_e} + |c_{v_0}(t)|^2 B_{v_0} \\ &+ \sum_{(v_e \neq v_e')} 2 c_{v_e}(t) c_{v_e'}(t) B_{v_e' v_e} \\ &\times {\rm Re}\left({\rm e}^{-{\rm i}2\pi \left[\frac{v_e - v_e'}{T_{\rm cl}(\bar v_e)} + \frac{(v_e - \bar v_e)^2 \pm (v_e' - \bar v_e)^2}{T_{\rm rev}(\bar v_e)} \right] t} \right) \\ &+ \sum_{v = v_0 - 1, v_0 + 1} 2 c_v(t) c_{v_0}(t) B_{v_0 v} {\rm Re}\left({\rm e}^{{\rm i}2\pi \frac{t}{T^{\rm int,ext}}} \right). \end{aligned} \tag{26}$$

The times appearing in (26) have the values: $T_{\rm cl}(\bar v_e) = T_{\rm vib}(\bar v_e) = 210$ ps, $T_{\rm rev}(\bar v_e) = 4\,200$ ps, and $T^{\rm int,ext} = 420$ ps. The sum $\sum_{(v_e \neq v_e')}$ is mainly directed by the evolution of $\Psi_e(R,t)$ described previously, and $\sum_{v = v_0 - 1, v_0 + 1}$ introduces the beating between the two wells with a period $T^{\rm int,ext}$ and contributes with large values $B_{v_0 v}$ at $B(t)$.

The minima of $B(t)$ and $P_i(t)$ appear when the population in the inner well approaches 0, which happens for a partial revival or fractional revival of the wavepacket at large distances. As we showed previously, for $t \approx T_{\rm rev}(\bar v)N/4$, so for $t \approx 1\,050$, 2 100, 3 150, 4 200, 5 250, 6 300, ... ps there is a "partial revival" of the packet at large distances, in the sense that it leaves the inner well for some period. We see that these values correspond effectively to the minima in $P_i(t)$ and $B(t)$.

On the other hand, for $t = T_{\rm rev}(\bar v)N_o/8$, with N_o odd integer, that means $t = 525$, 1 575, 2 625, 3 675, 4 725, 5 775 ps, etc., ${\rm Re}({\rm e}^{{\rm i}2\pi \frac{t}{T^{\rm int,ext}}}) = {\rm Re}({\rm e}^{{\rm i}5\pi/2}) = 0$, because $T_{\rm rev} = 10T^{\rm int,ext}$. So, the last term in the expression (26) implying beating between v_0-1 or v_0+1 and v_0 becomes 0. In the Figure 4 these values of time correspond to partial emptying of the inner well and minima in $P_i(t)$ and $B(t)$.

What can we learn from this analysis? We simply observe here the movement of a packet composed of a superposition of vibrational states formed in the external well, at an energy allowing tunneling to the inner well. The possibility of tunneling advanced by the stationary analysis is then confirmed, and moreover we identify an effect which can be called "efficiency" of tunneling. At –3 cm^{-1}, a maximum of 15% of the 0_g^- population is transferred to the inner well and $P_i \approx 7.5\% P_{0_g^-}$ during 6 000 ps. As expected, the efficiency is increased at –2.9 cm^{-1}, the maximum being of 30%, and the population in the inner well being doubled ($P_i \approx 15\% P_{0_g^-}$ during 6 000 ps). We can distinguish two regimes in the movement of the wavepackets: one of a strong separation of the packet in two parts, respectively located in the inner well and in the outer well at large distances ($R > 50a_0$), corresponding to maxima

of $P_i(t)$ and $B(t)$ (see for example the wavepackets for $t = 150$, 200 or 850 ps); in the other regime, the packet occupies the external well in a range of distances between 15 and $60a_0$ which encourage under-barrier transit between the two wells (for example, the packet at $t = 350$ ps). This second regime produces in Fig. 4b) values of $B(t)$ between $B_v^{\rm ex}$ and B_v^{e-t} (the rotational constant for $v_0 - 1$, $v_0 + 1$). The time-evolution combines the specific dynamics of a superposition of levels in the external well implying partial "revival" at large distances, and the beating between the two wells with a period $T^{\rm int,ext} \approx 420$ ps. The presence of the inner well level and the tunneling emphasizes the dephasing between terms with different energies and introduces an "irreversibility" in the evolution: Figures 4a and 4b show that after $T_{\rm rev} = 4\,200$ ps, the pattern starts to be modified. We have also identified a time elapsed until a maximal filling up or emptying of the inner well (from 0 to $P_i^{\rm max}$, and from B_v^{e-t} to $B_v^{\rm max}(t)$) which is between 50 and 100 ps.

5 Photoassociation and tunneling two channels: $a^3\Sigma_u^+ \longrightarrow 0_g^-(6s, 6p_{3/2})$

Our main purpose is a time-dependent analysis of the photoassociation when a cw laser is turned on at resonance with the energy region where tunneling occurs. As discussed in a previous paper [8], the choice of the initial state for a time-dependent propagation simulating photoassociation can be numerically problematic. We have performed photoassociation simulations using a Gaussian packet as initial state in the $a^3\Sigma_u^+$ channel, which is a valid representation for sufficiently high temperatures [8]. This means that $\Psi_\Sigma(R, 0)$ is defined as in formula (16), and $\Psi_{0_g^-}(R, 0) = 0$. The initial Gaussian $\Psi_\Sigma(R, 0)$ is chosen as being centered at the excitation point $R_e = R_0$ and having a very small initial momentum $p_0 = 0.012$ au, corresponding to a Maxwellian velocity distribution of cesium atoms at a temperature $T = 200$ μK. In order to confine the calculations on a reasonable spatial grid size, the width of the Gaussian is established at $\Delta R(0) = 7.5a_0$ in position or $\Delta p(0) = 0.066$ au in momentum, which corresponds to a temperature of 6 mK. Comparing with the real conditions of the photoassociation experiments, this localized representation of the initial state encourages a more rapid dynamics in the ground state $a^3\Sigma_u^+$, induced by the large momentum components of the initial packet. An interesting question is to which extent the ground state dynamics is influencing the excited state dynamics and *vice versa*.

The two channels being continuously coupled by light, and the coupling active only around the excitation point R_e, at a given time t the transfer between the ground and excited states is conditioned by the amount of population localized around this precise distance. Then the photoassociation dynamics of the two coupled channels varies a lot with the detuning, not only because of the change in the Franck-Condon factors (as it is well-known, the photoassociation efficiency increases by decreasing the detuning), but also because the distances of vibration are changed. Photoassociation into different excitation states is "an optical method for altering the interactions between ground-state atoms" [21]: even if not relative to the dynamics, this point was stressed in the last years due to the increased interest for a control of interactions in the ground state, important for the achievement of Bose-Einstein condensates. From the point of view of our present study, it is interesting to remark that the vibrational levels of 0_g^- state lying at about –3 cm^{-1}, close to the energy of tunneling, represent very different final states for photoassociation, susceptible to induce different dynamics in the ground triplet state, even if they are neighbouring vibrational levels. We shall probe this by modeling of the photoassociation in the 0_g^- double well for different detunings around 3 cm^{-1}, corresponding to excitation of $v_0 - 1$ (level of the outer well with tunneling), v_0 (inner well level with tunneling), and $v_0 + 2$ (outer well) vibrational levels. The excitation distances R_e for these levels are: $91.2a_0$, $92.3a_0$, and $94.3a_0$. The initial wavepackets on the triplet state being centered in $R_0 = R_e$ with the same initial momentum and width, the initial state is almost the same in all three cases. The coupling $\hbar\Omega$ due to cw laser field is also the same: results will be shown for $\hbar\Omega = 0.026$ cm^{-1}, corresponding to $I \approx 150$ W/cm^2 in linear polarisation ($T_{\rm Rabi} = 640$ ps). To see the differences for tunneling, we also consider a twice larger coupling $2\hbar\Omega$ ($I \approx 600$ W/cm^2 in linear polarisation, and $T_{\rm Rabi} = 320$ ps).

It can be expected that the tunneling will take place differently from the propagation in the 0_g^- alone, because now the packet in the double well proceeds from the photoassociation of two cold atoms with a cw-laser, meaning that not only it has very small kinetic energy, but a precise vibrational level of the 0_g^- double well is excited, and not a superposition of vibrational states.

The time-dependent Schrödinger equation (8) for the two coupled channels is solved numerically on a grid of length L (extending from $8.3a_0$ to $319a_0$, and having 8 192 points). A second grid, much smaller (2 048 points), continuing this main grid, is used to absorb the population which goes out from the interaction zone during the time-evolution. In fact, the second grid is useful only for the $a^3\Sigma_u^+$ channel, because a part of the initial Gaussian wavepacket spreads to large distances. Generally we tried to use a grid sufficiently large to keep total population constant on the main grid ($P_{\rm tot} = P_{0_g^-} + P_{^3\Sigma_u^+} = 1$) during a period as long as possible.

5.1 Resonant excitation of the level $v_0 - 1$ of the outer well

We consider now the photoassociation of two cold atoms by a cw-laser, tuned at $\hbar\Delta_{\rm L} = 3$ cm^{-1} relative to the $(6s + 6p_{3/2})$ asymptote, on resonance with the level $v_0 - 1$ lying at -2.984 cm^{-1} in the outer well. The coupling $\hbar\Omega = 0.026$ cm^{-1} ($T_{\rm Rabi} = 640$ ps) corresponds at $I \approx 150$ W/cm^2 in linear polarisation. The initial Gaussian wavepacket in the $^3\Sigma_u^+$ state is centered at $R_0 \approx 91a_0$ and has the initial energy -2.998 cm^{-1}.

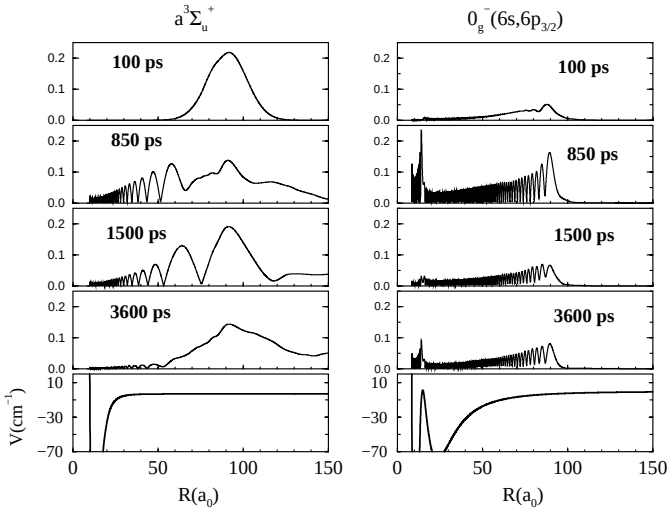

Fig. 7. Evolution of wavepackets on $a^3\Sigma_u^+$ (left column) and $0_g^-(6s, 6p_{3/2})$ (right column) channels, during modelized photoassociation at detuning $\hbar\Delta = 3\ \mathrm{cm}^{-1}$ (resonant excitation of the level $v_0 - 1$ of 0_g^-). The corresponding potentials are also shown.

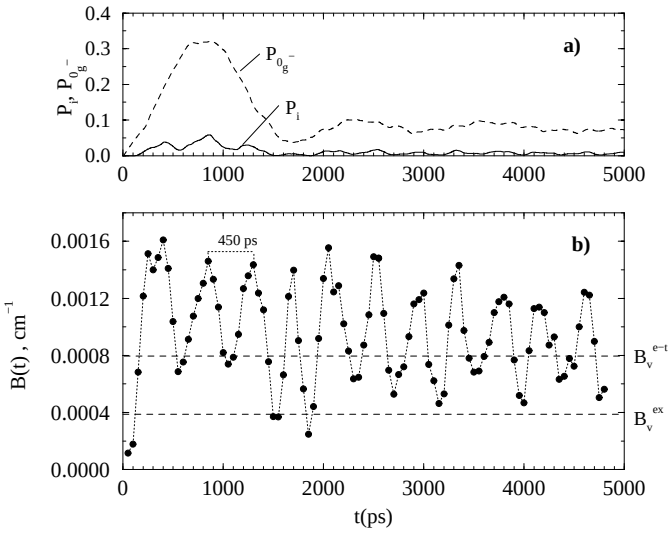

Fig. 8. Resonant excitation of level v_0-1 of 0_g^- ($\hbar\Delta = 3\ \mathrm{cm}^{-1}$). (a) Time variation of the population in the $0_g^-(6s, 6p_{3/2})$ potential ($P_{0_g^-}$, represented with dashed line) and in the inner well (P_i, full line). The total population $P_{\mathrm{tot}} = P_{^3\Sigma_u^+} + P_{0_g^-} = 1$. (b) Time variation of the $B(t)$ – "rotational constant of the wavepacket".

The important difference with the previous case is that only one vibrational level of the $0_g^-(6s, 6p_{3/2})$ outer well is excited, namely v_0-1, which tunnels to the inner well, as it can be seen in Figure 7 displaying the wavepackets evolution, and in Figure 8a showing the total population excited in the 0_g^- channel, $P_{0_g^-}(t)$, and the amount $P_i(t)$ which occupies the inner well. $P_{0_g^-}(t)$ increases in the first 850 ps, after which it begins to diminish and stabilizes at 8% of the total population. Trying to explain this behaviour, we find that the oscillation of about 1 600 ps which can be observed in the beginning is related to the movement of the $a^3\Sigma_u^+$ packet in the ground state, displayed in the left column of the Figure 7. The transfer of population from ground to excited state is taking place around $91a_0$, at the crossing point of the dressed potential curves which coincides here with the center of the initial packet on ground state. This transfer is stopped and inversed around 850 ps by the diminution of the population in the ground state around R_e. As we see in Figure 7, at $t = 850$ ps both packets have the same height at $R_e \approx 91a_0$ and the population is not longer transferred to 0_g^- (in strong field the transfer continues until the creation of a hole in the initial packet, which causes the inversion of population; it is not the case here, we are in a "weak field regime"). At 1 500 ps the $a^3\Sigma_u^+$ packet reaches again a maximum around R_e, and the population increases on the excited channel, but after 2 000 ps a regime of saturation is installed and the excited state population is stabilized around $P_{0_g^-} = 0.08P_{\mathrm{tot}}$. As a result, in the first 1 600 ps, the maximum population transferred to the inner well is 5% (it is remarkable that this represents $P_i = 0.16P_{0_g^-}$, the same percentage as in the one-channel propagation), but after 1 600 ps it stabilizes to very low value. Nevertheless, oscillations with a period of about 450 ps can be distinguished in the behaviour of $P_i(t)$ during all the evolution. Indeed, as it can be seen in Figure 8b, the "rotational constant" $B(t)$ has a remarkable simple behaviour, consisting of oscillations with a period of about 450 ps, close to the beating time between the two wells $T^{\mathrm{int,ext}} = T_{v_0-1,v_0} = 420$ ps. This simple oscillation is accounted for by formula (26), for the case in which we have only the levels $v_0 - 1$ and v_0. The domain of variation of $B(t)$ is also changed: most of the time $B(t)$ is much larger than rotational constants $B_v^{e-t} \approx 0.8 \times 10^{-3}\ \mathrm{cm}^{-1}$ of levels $v_0 - 1$, $v_0 + 1$, but far from the value $B_v^0 = 4.5 \times 10^{-3}\ \mathrm{cm}^{-1}$ of the inner well level v_0. The 0_g^- wavepacket is typically extending both in the inner and in the outer well.

5.2 Excitation of the level v_0 of the inner well: off-resonance excitation

Now we assume that a cw-laser with the same intensity is tuned ($\hbar\Delta_{\mathrm{L}} = 2.9\ \mathrm{cm}^{-1}$) off-resonance relative to the levels of the outer well, so that the photoassociation efficiency is expected to be low, but on-resonance with the level v_0 at $-2.9\ \mathrm{cm}^{-1}$ in the inner well. In fact the vibrational level v_0 of the inner well can be viewed as tunneling from the inner to the outer well, and having an nonnegligible part of its wavefunction in the external well, which makes possible its excitation from large distances. The initial state is represented by a wavepacket in the $a^3\Sigma_u^+$ electronic state having the same characteristics as before, but centered at $\approx 92a_0$. The initial energy is $-2.898\ \mathrm{cm}^{-1}$ relative to the $(6s + 6p_{3/2})$ asymptote.

As it is shown in Figure 9a, the efficiency of the photoassociation process is poor: less than 10% of the population is transferred to the excited 0_g^- state. Nevertheless, the transfer to the inner well is much more efficient

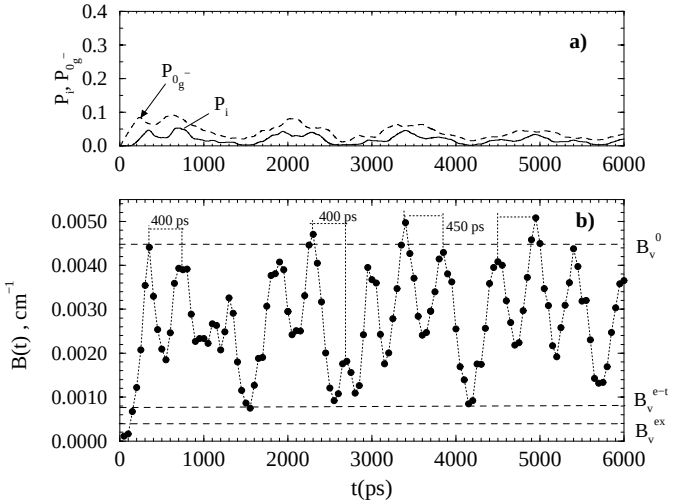

Fig. 9. Excitation of the level v_0 of the inner well ($\hbar\Delta_{\rm L} = 2.9$ cm^{-1}). (a) Time variation of the population $P_{0_g^-}$ in the $0_g^-(6s, 6p_{3/2})$ potential (dashed line) and in the inner well (P_i, full line). (b) Time variation of $B(t)$ – "rotational constant" of the 0_g^- wavepacket.

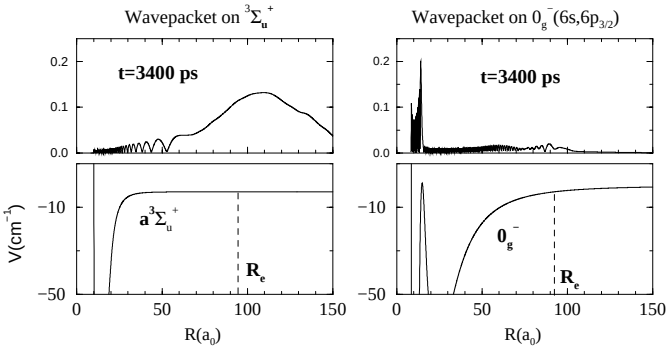

Fig. 10. Excitation of the level v_0 of the inner well by photoassociation at large distance R_e. Wavepackets on $a^3\Sigma_u^+$ (left column) and on $0_g^-(6s, 6p_{3/2})$ (right column) channels and corresponding potentials.

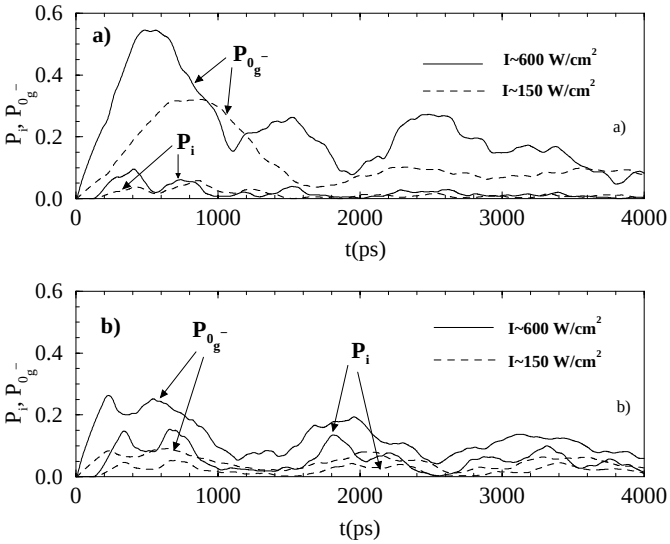

Fig. 11. Population on 0_g^- channel, increasing the laser intensity (coupling two times bigger). (a) Resonant excitation of $v_0 - 1$ ($\Delta = 3$ cm^{-1}), (b) excitation of the level v_0 of the inner well ($\Delta = 2.9$ cm^{-1}).

than in the previous case. The population P_i in the inner well oscillates between 5% of the total population and 0 (during 6 000 ps, $\approx 2.5\%$ of the total population is in the inner well). The oscillatory behaviour of the $P_{0_g^-}(t)$ and $P_i(t)$ with a period of about 1 400 ps suggests a "strong field effect", in the sense that the inner well population is more sensitive at the laser intensity than before, when the external level $v_0 - 1$ was excited. Indeed, we did calculations for a coupling which is twofold, $2\hbar\Omega$ (the intensity is $I \approx 600$ W/cm^2 in linear polarisation), and the results are displayed in Figure 11b. It is obvious that the efficiency of the tunneling is strongly increased by increasing the laser intensity. This is not true for the resonant excitation of $v_0 - 1$: in Figure 11a it can be observed that the population transferred in the 0_g^- excited state markedly depends upon the laser intensity, but the tunneling efficiency is not really increased (as we see for an intensity of 600 W/cm^2, after 2 000 ps). Figure 11b makes clear that the "slow oscillations" of $P_{0_g^-}(t)$ and $P_i(t)$ keep approximately the same period, between 1 200 and 1 400 ps, even for a double intensity of the field. This oscillant behaviour illustrate the exchange of population with the ground triplet state and it is certainly strongly influenced by the movement of the $a^3\Sigma_u^+$ packet. Besides these large oscillations, the "beating oscillations" of about 400−450 ps due to tunneling can be observed not only in the inner well population $P_i(t)$, but also on the whole 0_g^- population $P_{0_g^-}(t)$, at both intensities. This means that tunneling influences the population transfer at large distances during photoassociation, as it determines the vibrational movement in the double well.

The 0_g^- packet excited in the photoassociation is typically localized in the inner well (see Fig. 10), as it is shown by $B(t)$ (Fig. 9b), whose values are much bigger than those of rotational constants for $v_0 - 1$, $v_0 + 1$. The value $B_v^0 = 4.5 \times 10^{-3}$ cm^{-1} of the inner well level v_0 is reached during the time-evolution.

These results show that the inner well can be populated either by "direct excitation" of the inner well level v_0, or by exciting one of the $v_0 - 1$, $v_0 + 1$ neighbouring levels belonging to the outer well, but manifesting also tunneling. The population of the inner well depends on the photoassociation efficiency, which is bad for a laser tuned off-resonance with an external well level. In the competition between photoassociation efficiency and tunneling efficiency, we find that tuning the laser at resonance with a level in the external well, as close as possible to the tunneling energy, yields a large photoassociation probability, and a small tunneling probability; tuning the laser at resonance with the vibrational level in the inner well yields a small photoassociation probability, but a large tunneling probability. The two choices give equivalent results during the first 1 000 ps, but the second choice is much more

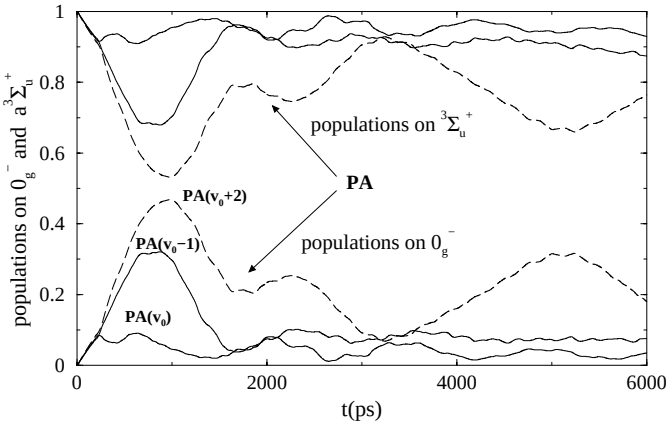

Fig. 12. Time-dependent evolutions of populations on $a^3\Sigma_u^+$ and 0_g^- channels in modelized photoassociation (coupling $\hbar\Omega = 0.026\ \mathrm{cm}^{-1}$) for different excited levels of 0_g^-: v_0-1 ($-3\ \mathrm{cm}^{-1}$), v_0 ($-2.9\ \mathrm{cm}^{-1}$), and v_0+2 ($-2.7\ \mathrm{cm}^{-1}$). The initial packet in the ground state is almost the same (after 5 000 ps, the $a^3\Sigma_u^+$ populations begin to leave the main grid).

efficient on a larger timescale and also very sensitive at the laser intensity.

Before ending this section, we find interesting to illustrate the remarks made in the beginning about how different can be the dynamics of the system reaching close photoassociation resonances. In Figure 12 we show results obtained for v_0-1, v_0 (outer and inner well levels with tunneling) and v_0+2 (which is a "pure" outer well level). The coupling is the same, and the initial ground state can also be considered the same, as the excited states are really very close one to the other. It is the quality of the final states that induces different dynamics of the system and consequently changes the behaviour in the ground triplet state. In all these three cases there is a first oscillation of the populations having almost the same period, around 1 600 ps, which can be explained by the movement of the packet in the ground state. Subsequently, their evolutions become completely different. The marked oscillatory behaviour in the v_0+2 excitation indicates that the "same field" is felt as a stronger one with the decrease of the detuning.

6 Conclusion

The paper contains a time-dependent analysis of the tunneling effect observed in the cesium photoassociation experiments when vibrational levels of the $0_g^-(6s, 6p_{3/2})$ double well potential are populated at large interatomic distances, after absorption of a photon by a pair of cold cesium atoms. The interest of the reaction lies in the production of ultracold molecules in low vibrational levels. Previous works [7,6] have shown that the observed spectrum contains the evidence for tunneling to the inner well at detunings of -2.14 (G_1) and $-6.15\ \mathrm{cm}^{-1}$ (G_2), and that the experimental results could be reproduced by stationary calculations taking into account the coupling at small distances between $0_g^-(6s, 6p_{3/2})$ and $0_g^-(6s, 5d)$, and using potentials slightly modified from *ab initio* calculations of Meyer's group at short distances, matched to asymptotic calculations of Marinescu and Dalgarno. In the present work a simplified model has been considered where the coupling with the $0_g^-(6s, 5d)$ channel in the inner region is not considered, which implies that we study only one (G_1) of the two structures, which is due to the presence in the $0_g^-(6s, 6p_{3/2})$ potential of a inner well level v_0 at $-2.9\ \mathrm{cm}^{-1}$, for which tunneling is important. In fact the tunneling occurs not only for level v_0 which has a wavefunction mainly located in the inner well, but also for the neighbouring levels (v_0-1) and (v_0+1), mainly located in the outer well.

We first have studied the tunneling effect alone, by considering the evolution of a wavepacket with energy close to v_0, and located in the external well around the outer turning point at this energy. The time evolution of a packet made by a superposition of vibrational levels including (v_0-1, v_0, v_0+1) shows beating between the two wells due to tunneling and a partial "revival" phenomenon bringing periodically the population at large distances. We identify characteristic times corresponding to vibration in the external well (200−250 ps), beating between the two wells (420 ps), and fractional revivals at $t = NT_{\mathrm{rev}}(v_0-1)/4$, N integer, leading to emptying of the inner well at regular intervals. The population of the inner well can reach a maximum of 30% for a wavepacket centered at the energy of the level v_0.

In a second part we simulate the photoassociation reaction $a^3\Sigma_u^+ \rightarrow 0_g^-(6s, 6p_{3/2})$, by considering that a linearly polarised cw-laser with intensity of about 150 W/cm^2 is turned on at time $t = 0$, coupling the two electronic states at a detuning allowing the observation of tunneling. This laser coupling can be viewed as a Rabi cycling with a period of 640 ps, which determines the exchange of population between the continuum of the $a^3\Sigma_u^+$ electronic state and a vibrational level of the $0_g^-(6s, 6p_{3/2})$. For the levels v_0-1, v_0+1 of the external well with vibrational periods of 200−250 ps, this coupling can be qualified as a weak one, the packets having time enough for several vibration periods during a "Rabi period". We simulated photoassociation at different detunings, in order to populate either a level (v_0-1) or (v_0+1) of the external well (resonant excitation), or the v_0 level of the inner well ("off-resonance" excitation). The wavefunction of this latter level is exponentially decreasing in the outer well. In the first case the photoassociation reaction is efficient, transferring up to 30% of the population in the excited state, but the tunneling probability is small. In the second case, the tunneling probability is large, so that despite the poor efficiency of the photoassociation process, transferring less than 10% of the initial population in the excited state, up to 5% of the population can still be transferred into the inner well, with a strong probability of forming ultracold molecules in low vibrational levels by spontaneous emission. For the excitation "off-resonance" of the v_0 level, the results depend markedly of the laser intensity, which could be used to control the inner well population. It is also remarkable that in the v_0 excitation the exchange of population

between the two channels ($P_{0_g^-}(t)$ and $P_{^3\Sigma_u^+}(t)$) are modulated in time by the beating period of 420 ps implying tunneling between the two wells.

Our observation that the inner well is populated by the direct excitation of a level v_0 of the inner well, with evanescent wave function in the region of the outer well, helps to a better understanding of the experimental spectrum discussed in reference [6]. The photoassociation process is not very efficient in this case, due to a poor overlap with the wavefunction describing two colliding ground state atoms. Previous work did not explain why only certain rotational lines of the structures G_1, G_2 (assigned to the coupled inner wells $0_g^-(6s, 6p_{3/2})$ and $0_g^-(6s, 5d)$) are "giant". From the spectrum published in reference [6] it can be seen that the intense lines are observed for J values where the tunneling level in the inner well coincides with a $v_{\rm ext}$ level in the outer well. So the giant lines of the experimental spectrum, manifesting an important occupation of the inner well and formation of cold molecules in low vibrational levels, are obtained when both conditions of photoassociation efficiency and tunneling efficiency are fulfilled. This will be discussed in more details in a forthcoming paper, where the calculations are including coupling with the $0_g^-(6s, 5d)$ channel and J-dependence, as well as spontaneous emission to the ground triplet state. Such calculations show that the present simplified model is accounting for all the physical effects. They will give quantitative predictions for the formation rate of ultracold molecules in the $a^3\Sigma_u^+$ lower triplet state.

In the beginning of this work, we addressed a question about the possibility of observing a "tunneling time" in our results. It is no doubt that in the present problem the barrier is crossed "very rapidly" by fast components of the wavepacket, but we are more interested in the evolution of the inner well population, depending on the dynamics of the wavepacket that is moving in the external well. We find that when we study the motion of a wavepacket made by a superposition of states, a "tunneling time" of 50−100 ps leads to a maximal occupation of the inner well. But in the photoassociation experiment, when a $0_g^-(6s, 6p_{3/2})$ level is excited by a cw photoassociation laser, the relevant time is the beating time of 420 ps between the two wells, determined by the energy splitting between v_0 and $v_0 - 1$ (or $v_0 + 1$).

Future work should include photoassociation with a pulsed laser, where several levels are populated simultaneously, and propose a way of substantially increasing the formation rate of ultracold molecules in low vibrational levels of the ground triplet state, *i.e.* "vibrationally cold molecules". Pump-probe experiments should be particularly interesting in the present problem.

The authors are grateful to M. Aymar, E. Luc-Koenig, O. Dulieu and R. Kosloff for critical reading of the manuscript and stimulating discussions. This work benefited by a cooperation agreement between CNRS and Academy of Sciences of Romania.

References

1. A. Fioretti, D. Comparat, A. Crubellier, O. Dulieu, F. Masnou-Seeuws, P. Pillet, Phys. Rev. Lett. **80**, 4402 (1998)
2. T. Takekoshi, B.M. Patterson, R.J. Knize, Phys. Rev. Lett. **81**, 5105 (1999)
3. N. Nikolov, E.E. Eyler, X.T. Wang, J. Li, H. Wang, W.C. Stwalley, Ph. Gould, Phys. Rev. Lett. **82**, 703 (1999)
4. C. Gabbanini, A. Fioretti, A. Lucchesini, S. Gozzini, M. Mazzoni, Phys. Rev. Lett. **84**, 2814 (2000)
5. H.R. Thorsheim, J. Weiner, P.S. Julienne, Phys. Rev. Lett. **58**, 2420 (1987)
6. M. Vatasescu, O. Dulieu, C. Amiot, D. Comparat, C. Drag, V. Kokoouline, F. Masnou-Seeuws, P. Pillet, Phys. Rev. A **61**, 044701 (2000)
7. A. Fioretti, D. Comparat, C. Drag, C. Amiot, O. Dulieu, F. Masnou-Seeuws, P. Pillet, Eur. Phys. J. D **5**, 389 (1999)
8. M. Vatasescu, O. Dulieu, R. Kosloff, F. Masnou-Seeuws, Phys. Rev. A **63**, 033407 (2001)
9. R. Landauer, Th. Martin, Rev. Mod. Phys. **66**, 217 (1994)
10. D.H. Kobe, H. Iwamoto, M. Goto, V.C. Aguilera-Navarro, Phys. Rev. A **64**, 022104 (2001)
11. E.H. Hauge, J.P. Falck, T.A. Fjeldly, Phys. Rev. B **36**, 4203 (1987)
12. M.S. Marinov, B. Segev, Phys. Rev. A **55**, 3580 (1997)
13. N. Spies, Ph.D. thesis, Fachbereich Chemie, Universität Kaiserslautern, 1989
14. M. Marinescu, A. Dalgarno, Phys. Rev. A **52**, 311 (1995)
15. V. Kokoouline, O. Dulieu, R. Kosloff, F. Masnou-Seeuws, J. Chem. Phys. **110**, 9865 (1999)
16. M. Vatasescu, Ph.D. thesis, Université Paris-Sud, 1999
17. R. Kosloff, Annu. Rev. Phys. Chem. **45**, 145 (1994)
18. R. Kosloff, *Dynamics of Molecules and Chemical Reactions*, edited by R.E. Wyatt, J.Z. Zhang (Marcel Dekker, 1996), pp. 185–230
19. I.Sh. Averbukh, N.F. Perelman, Usp. Fiz. Nauk **161**, 41 (1991); I.Sh. Averbukh, N.F. Perelman, Phys. Lett. A **139**, 449 (1989)
20. D.K. Roy, *Quantum Mechanical Tunneling And Its Applications* (World Scientific Publishing, Singapore, 1986), pp. 19–36
21. J.M. Gerton, B.J. Frew, R.G. Hulet, Phys. Rev. A **64**, 053410 (2001)